ORGANIC CHEMISTRY FRONTIERS

RESEARCH ARTICLE

View Article Online
View Journal | View Issue

Cite this: *Org. Chem. Front.*, 2024, **11**, 5754

The *N*-biphenyldihydroisoquinolinium scaffold as a novel motif for selective fluorimetric detection of quadruplex DNA†‡

Denisa Soost, [a] Gerhard Bringmann [b] and Heiko Ihmels *[a]

Received 28th June 2024,
Accepted 26th August 2024

DOI: 10.1039/d4qo01193g

rsc.li/frontiers-organic

The spectroscopic investigation of the DNA-binding properties of (*S*)-6,8-dimethoxy-2-(4′-methoxy-[1,1′-biphenyl]-4-yl)-1,3-dimethyl-3,4-dihydroisoquinolin-2-ium revealed the cationic donor–acceptor-substituted biaryl unit as a promising motif for selective fluorimetric detection of particular quadruplex DNA (G4-DNA) forms. The title compound exhibits the characteristic solvent-dependent dual emission of biaryl fluorophores; however, the emission quantum yields are very low ($\Phi_{fl} \leq 0.01$) because of radiationless deactivation of the excited state by conformational changes. In contrast, the emission intensity of the biaryl derivative increases by a factor of 2–10 on association with G4-DNA (K_B = 8 × 10^4 M^{-1}–4 × 10^5 M^{-1}), because the structural relaxation of the exited ligand is suppressed in the binding site. The signal pattern of the dual emission, specifically the relative contribution of each band, varies with the different G4-quadruplex forms **22AG**, **c-kit**, **c-myc**, **c-kras**, and **h-ras1**, most likely caused by the different dynamic flexbility of the ligand in the distinct binding sites. These effects enable the fluorimetric identification of sterically constrained binding sites, such as in **c-kit** and **h-ras1**, even with the naked eye.

Introduction

The selective staining and detection of nucleic acids is an important bioanalytical technique in chemistry and biology.[1] For this purpose, organic fluorescent probes figure as valuable and versatile tools.[2] Specifically, dyes with a very low emission intensity that increases upon association with the target analyte, often referred to as fluorescent "light-up probes", have proven to be very useful and provide valuable chemosensors for the fluorimetric detection of DNA and similar targets *in vitro* and *in vivo*.[3] In this context, especially the non-canonical quadruplex DNA (G4-DNA) is an important target.[4] Quadruplex DNA is formed upon folding and assembly of guanine-rich DNA strands to a stack of usually three neighboring guanine quartets.[5] The structures of quadruplex DNAs vary depending mainly on the particular sequence of the parent single strand(s).[6] Most importantly, G4-DNA structures have essential biological functions, for example in the promoter regions of oncogenes, which influence the growth of cancer cells,[7] or in the single-stranded overhang of telomeric DNA.[8] Therefore, G4-DNA is an attractive target for the development of fluorescent probes that enable the detection and monitoring of this DNA form.[9] Indeed, various fluorescent probes have already been developed that may be used to detect G4-DNA structures and to differentiate them from other DNA forms[10] *in vitro*[11] and in cells.[12] Hence, it has been demonstrated that suitable cationic dyes, for example distyrylpyridinium derivatives such as **1**, bind selectively to particular target G4-DNA structures and that this complex formation is accompanied by a characteristic, G4-DNA-specific fluorescence light-up effect (Scheme 1).[13] As another notable example, the cyanine dye **2** exhibits a strong fluorescence light-up effect upon selective association with the G4-DNA form **c-myc** (Scheme 1),[14] which has been used to identify and distinguish this quadruplex form from other nucleic acid structures.[15] But, despite the highly favorable detection properties of these and other[2,13] fluorescent probes, there is still demand for novel approaches and for structural features that enable the selective detection of G4-DNA. Thus, there are, so far, only few examples of fluorescent probes available that are able to distinguish different topologies of G4-DNA with sufficient selectivity.[16] At the same time, it appears that selectivity is more easily accomplished for some G4-DNA forms, *e.g.* for **c-myc**,[14,15] whereas fluorescent probes for others, such as **c-kit**,[17] are still rare. Against this background, we report the coincidental

[a]*Department of Chemistry – Biology, and Center of Micro- and Nanochemistry and (Bio-)Technology (Cμ), University of Siegen, Adolf-Reichwein-Str. 2, 57068 Siegen, Germany. E-mail: ihmels@uni-siegen.de*
[b]*Institute of Organic Chemistry, University of Würzburg, Am Hubland, 97074 Würzburg, Germany*

† Dedicated to Prof. Dr. Frank Würthner on the occasion of his 60th birthday.
‡ Electronic supplementary information (ESI) available. See DOI: https://doi.org/10.1039/d4qo01193g

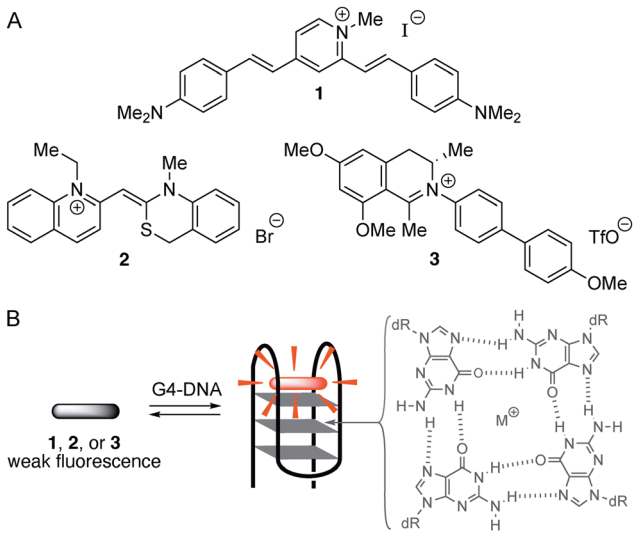

Scheme 1 (A) Structures of distyrylpyridinium and cyanine dyes **1** and **2** and of the biphenyl-substituted 3,4-dihydroisoquinolin-2-ium **3**. (B) Schematic representation of the fluorescence light-up effect of ligands upon binding to G4-DNA; grey: structure of a guanine quartet, dR = deoxyribose residue of the DNA backbone.

observation of the selective fluorimetric response of an *N*-biphenyldihydroisoquinolinium fluorophore upon binding to G4-DNA, which may contribute to the search for novel functional features of G4-DNA-targeting fluorescent probes. During our studies of the DNA-binding properties of dihydroisoquinolinium-based natural products,[18] we have noticed that the very weakly fluorescent cationic biphenyl-substituted derivative **3** showed a distinct fluorescence in the presence of nucleic acids, especially pronounced with G4-DNA. Therefore, we investigated the photophysical and the DNA-binding properties of this particular biphenyl derivative. And we will demonstrate herein that, indeed, this compound is a promising starting point for the development of G4-DNA-selective fluorescent probes.

Results and discussion

For a first orientation, the absorption and emission properties of biphenyl **3** were investigated in different solvents (Fig. 1 and

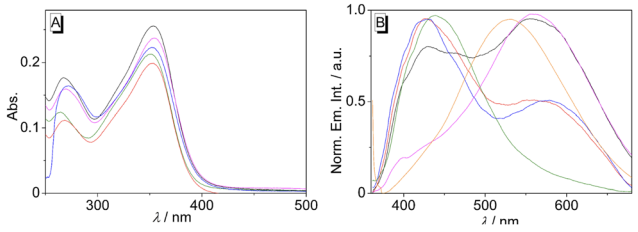

Fig. 1 Absorption (c = 10 μM) (A) and normalized emission spectra (B) (λ_{ex} = 350 nm) of **3** in H_2O (green), DMSO (blue), MeOH (black), EtOH (magenta), MeCN (red), and glycerol (orange).

Table 1 Absorption and emission properties of compound **3** in different solvents

Solvent	λ_{abs}[a]/nm	ε[b]/L mol^{-1} cm^{-1}	λ_{fl}[c]/nm	Φ_{fl}[d]
H_2O	350 (264)	21 300	439	<0.01
DMSO	352 (272)	22 280	428 (580)	0.01
MeOH	353 (267)	25 532	555 (429)	<0.01
EtOH	354 (269)	23 713	560	0.01
MeCN	352 (268)	19 849	426 (552)	<0.01

[a] Long-wavelength absorption maximum; c = 10 μM. [b] Molar extinction coefficient. [c] Emission maximum; λ_{ex} = 350 nm. [d] Fluorescence quantum yield relative to anthracene in cyclohexane (Φ_{fl} = 0.36). The smaller maximum is given in parantheses.

Table 1). The absorption spectra of compound **3** are almost independent of the solvent, and the long-wavelength maxima only changed in a small range, from 350 nm in water to 354 nm in EtOH (Fig. 1A). In contrast, the fluorescence properties of compound **3** were found to depend on the solvent (Fig. 1B). While in water, a blue-shifted emission maximum was detected at 439 nm, a red-shifted maximum at 560 nm was found in EtOH. At the same time, dual emission of biphenyl **3** was observed in MeOH, MeCN, and DMSO, namely with two distinct emission bands at 352–353 nm and 556–580 nm (Fig. 1B and Table 1). In all employed solvents the emission quantum yields of **3** are very low ($\Phi_{fl} \leq 0.01$, Table 1).

Dual emission has been frequently observed in fluorescent biphenyl derivatives that are integrated in a donor–acceptor system. And it is commonly explained by the dynamic photophysical processes in the excited state and the resulting different emitting excited species.[19] Specifically, the excitation induces an intramolecular charge transfer (CT), which is often referred to as charge shift (CS) in the case of ionic chromophores, and to conformational changes in the excited state leading to twisted (TICT) or planar structures (PICT).[19b,20] Accordingly, the emission properties of compound **3** are also influenced by the donor–acceptor interplay between the electron-donating methoxy group and the electron-withdrawing iminum functionality, in combination with the conformational changes of the biphenyl unit. Thus, compound **3** showed the expected emission band of a biphenyl chromophore at around 435 nm, which was assigned to the locally excited (LE) state, most likely formed after conformational change to an almost planar structure and a resonance-type excited state (Scheme 2).[20f] After further rotation around the biaryl axis, the TICT/CS state is formed with an almost perpendicular biphenyl structure, which results in the red-shifted emission band at *ca.* 550 nm (Scheme 2).[20f,21] Apparently, these two states are stabilized or destabilized to a different extent by several solvent properties, because there is no obvious relationship between the formation of the emission bands with the solvent parameters.[20c,22] As the fluorescence quantum yields are very low in all tested solvents, an additional non-radiative deactivation of the excited state obviously takes place with high efficiency, which may be caused by torsional relaxation around the biphenyl bond or around the C_{ar}–N or the C_{ar}–O bond of

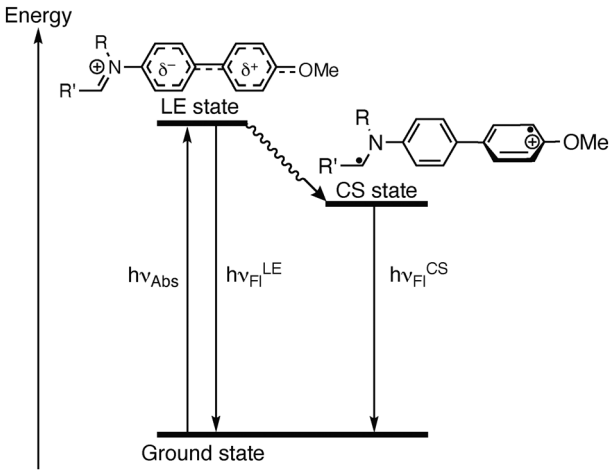

Scheme 2 State diagram of the photoexcitation and deactivation pathways of the *N*-biphenyldihydroisoquinolinium **3**.

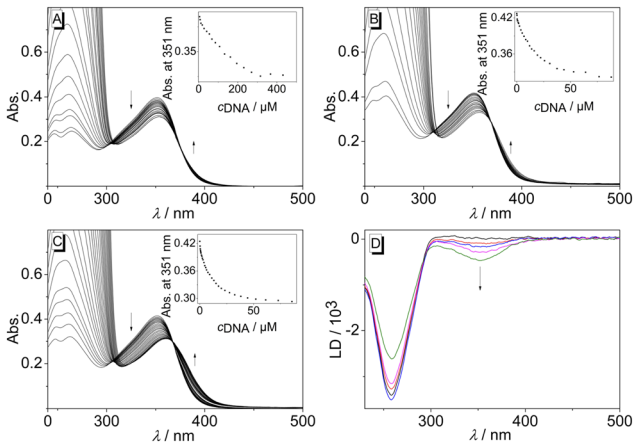

Fig. 2 Photometric titration of **3** (c = 20 μM) with ct DNA (A) in BPE buffer (c_{Na^+} = 16 mM, pH = 7.0), and with **22AG** (B) and **c-kit** (C) in K-phosphate buffer (c_{K^+} = 95 mM, pH = 7.0). The arrows indicate the development of the absorption bands during the titration. Inset: plot of the absorption at λ = 351 nm *versus* c_{DNA}. D: LD spectra of **3** in the presence of ct DNA (c = 20 μM) in BPE buffer (c_{Na^+} = 16 mM, pH = 7.0) at LDR = 0.0 (black), 0.2 (red), 0.5 (blue), 1.0 (magenta), 1.5 (green).

the donor and acceptor substituents.[23] To verify this assumption, the fluorescence spectra were recorded in media with different viscosity, namely in glycerol/water with increasing glycerol content (Fig. S4, *cf.* ESI‡), because the viscosity of the solvent has a considerable effect on the rate of conformational changes, thus, on the emission quantum yield of excited molecules.[24] Indeed, it was observed that in glycerol/water mixtures with higher viscosity, namely with glycerol fraction >40%, the emission intensity of **3** increased significantly with increasing glycerol content (Fig. 1B and Fig. S4 *cf.* ESI‡). Usually, this observation indicates a non-radiative deactivation of the excited state by conformational changes, such as torsional relaxation,[25] because in highly viscous glycerol the conformational changes are slowed down and emission becomes competitive.[26] Hence, torsional relaxation from either the LE state or the TICT/CS state of **3** to a non-emitting conformer most likely contributes to a significant extent to the non-radiative deactivation of the excited state.

The interactions of biphenyl **3** with calf thymus (ct) DNA, as a typical duplex DNA structure, and with representative quadruplex DNA (G4-DNA) forms **22AG**, **c-kit**, **c-kras**, **c-myc**, and **h-ras1** were investigated. These G4-DNA forms relate to specific, biologically relevant DNA sequences and have a unique sequence and structure, as defined by the arrangement of the G-quartets and loop regions.[27] The ligand-DNA interactions were monitored by photometric and fluorimetric titrations in aqueous buffer solutions. In almost all cases, a continuous decrease of the absorption maxima of compound **3** at 351 nm and a slight red shift ($\Delta\lambda_{ctDNA}$ = 3 nm, $\Delta\lambda_{\mathbf{22AG}}$ = 6 nm, $\Delta\lambda_{\mathbf{ckit}}$ = 9 nm) were observed upon addition of DNA (Fig. 2A, B, C and Fig. S1, *cf.* ESI‡). This effect was most pronounced upon addition of G4-DNA **c-kit**. Moreover, during titrations with G4-DNA, an isosbestic point was formed at 365 nm, whereas with ct DNA an initially formed isosbestic point faded during titration. The binding isotherms derived from the photometric DNA titrations of compound **3** were used to determine the binding constants K_b (Table 2 and Fig. S2, *cf.* ESI‡),[28] which revealed moderate binding affinities towards ct DNA (K_{ct} = 1.3×10^4 M^{-1}) and to G4-DNA ($K_{\mathbf{22AG}} = 7.6 \times 10^4$ M^{-1}; $K_{\mathbf{ckit}} = 1.6 \times 10^5$ M^{-1}; $K_{\mathbf{ckras}} = 1.8 \times 10^5$ M^{-1}, $K_{\mathbf{cmyc}} = 4.3 \times 10^5$ M^{-1}, $K_{\mathbf{hras1}} = 3.1 \times 10^5$ M^{-1}). However, the fitting curves of the binding isotherms of ct DNA, **c-kras**, and **h-ras1** showed deviations, presumably because of heterogeneous binding at relatively high or low ligand loading on the DNA. To further assess the binding mode of compound **3** with duplex DNA, the DNA-ligand complexes were analyzed by linear dichroism (LD) spectroscopy in the hydrodynamic field of a rotating cuvette.[29] In the presence of ct DNA, a negative LD signal between 300 nm and 400 nm was observed, that is in a range where only the ligand **3** absorbs. And the intensity of these LD bands

Table 2 Binding constants, K_b, of compound **3** with ct DNA and G4-DNA, and shifts of melting temperature, ΔT_m, of G4-DNA in the presence of **3**

	ct DNA	**22AG**[a]/**F21T**[b]	**c-kit**[a]/**FkitT**[b]	**c-kras**[a]/**FkrasT**[b]	**c-myc**[a]/**FmycT**[b]	**h-ras1**
K_b[a]/10^4 M^{-1}	1.3	7.6	16	18	43	31
ΔT_m[b]/°C	[c]	6	3	6	2	[c]

[a] Binding constant determined from photometric titrations with **22AG**, **c-kit**, **c-kras**, **c-myc**, and **h-ras1**. [b] Determined from fluorimetric analysis of dye-labeled oligonucleotides; estimated error ±0.5 °C. **F21T** = fluo-$G_3(TTAG_3)_3$-tamra, **FkitT** = fluo-$AG_3AG_3CGCTG_3AG_2AG_3$-tamra, **FmycT** = fluo-$TGAG_3TG_3TAG_3TG_3TA$-tamra, **FkrasT** = fluo-$AG_3CG_2TG_2A_2GAG_3A$-tamra, fluo = fluorescein, tamra = tetramethylrhodamine. [c] Not determined.

increased with increasing ligand-to-DNA ratio (LDR) (Fig. 2D). At the same time, the intensity of LD bands of the DNA bases decreased during the titration.

Overall, the photometric analyses indicated the association of the biphenyl **3** with nucleic acids. In particular, the changes in the absorption spectrum, namely hypochromism and the red shift of the absorption bands, are characteristic features of ligands that bind to duplex DNA[30] or G4-DNA.[31] Moreover, there are no large differences between the binding constants with the employed nucleic acids, which showed that there is no prounounced binding selectivity of the ligand towards a particular DNA form. In the case of duplex DNA, the additional LD-spectroscopic studies indicated an intercalation of the ligand, as confirmed by the negative LD bands of the ligand, which are characteristic of DNA intercalators.[32] Accordingly, the observed binding constant of **3** with ct DNA is in a range commonly observed for cationic DNA binders.[33] In contrast, the affinity of this ligand towards G4-DNA is relatively low as compared with the ones of known cationic ligands, which usually have binding constants of $K_b > 10^5$ M^{-1}.[34] In most cases, ligands that intercalate into duplex DNA tend to bind with G4-DNA by terminal π stacking to the quadruplex unit.[35] Therefore it is assumed that the ligand **3** binds with essentially the same binding mode to **c-kit**, **c-kras**, **c-myc**, and **h-ras1**, and that the low binding constants reflect a somewhat hindered fit of the ligand structure to the binding site. The latter may be caused by the three-dimensional steric demand of the ligand as it does not have the required planar structure.

In addition, the stabilization of the dye-labeled G4-DNA forms **F21T**, **FkitT**, **FkrasT** and **FmycT** towards thermally induced unfolding after binding of ligand **3** was investigated by thermal DNA-denaturation experiments (Table 2 and Fig. S4, *cf.* ESI‡).[36] Analysis of the melting temperature after ligand binding revealed a moderate stabilization of the quadruplex forms **F21T** (ΔT_m = 6 °C) and **FkrasT** (ΔT_m = 6 °C), whereas **FkitT** (ΔT_m = 3 °C) and **FmycT** (ΔT_m = 2 °C) were only slightly stabilized under the same conditions. These results indicated that upon binding the ligand **3** stabilizes the G4-DNA forms to a different extent depending on their topology. Notably, the shifts of the melting temperatures, ΔT_m, of the different G4-DNA forms in the presence of ligand **3** do not correlate well with the binding constants. This apparent contradiction has been observed frequently during studies of ligand-quadruplex interactions and may be explained by different dependencies of equilibrium constants and Gibbs free energies on the temperature,[6a] specifically as the binding constant was determined at temperatures below the respective DNA melting temperature. Furthermore, it was shown exemplarily that the stabilization of the G4-DNA **FkitT** by ligand **3** did not significantly change in the presence of the double-stranded DNA **ds26** [$d(CA_2TCG_2ATCGA_2T_2CGATC_2GAT_2G)$; ($\Delta\Delta T_m$ = −0.8 °C)], which indicated that the ligand binds selectively to the G4-DNA in competition with duplex DNA.[37,38]

To assess the influence of the association of ligand **3** with DNA on its emission properties, fluorimetric titrations with duplex and quadruplex DNA were conducted. In aqueous buffer solution, compound **3** showed a weak, hardly detectable emission band with a maximum at 460 nm. Upon addition of ct DNA, **22AG**, **c-kit**, **c-kras**, **c-myc**, and **h-ras1**, the emission intensity of the bound ligand **3** increased; however, the development of the emission bands varied distinctly with the different DNA forms (Fig. 3A, B, C and Fig. S1, *cf.* ESI‡). Specifically, the contribution of the two emission maxima resulting from the dual fluorescence of the ligand **3** (see above) depends on the respective DNA form. Upon addition of ct DNA, only one clear emission band developed with a maximum at 530 nm and with an increase of emission intensity by a factor of 2 (at ligand : DNA = 2), whereas the band at *ca.* 460 nm remained very weak. A similar development of the red-shifted fluorescence band at 535–538 with an intensity increased by a factor of 4–5 was observed with G4-DNA **22AG**, **c-kras**, **c-myc**, respectively. But in these cases, the intensity of the initial blue-shifted band also gradually increased, albeit to a smaller extent than the red-shifted band. In sharp contrast, the addition of **c-kit** and **h-ras1** to compound **3** led to a much stronger increase of the emission intensity of the blue-shifted band at 431 nm (**c-kit**) and 450 nm (**h-ras1**) by a factor of 5 and 10 (at ligand : DNA = 2), along with the rise of the red-shifted band with smaller intensity. In each case, the fluorescence light-up effect of the ligand **3** upon addition of DNA can be followed by the naked eye (Fig. 3). Moreover, the solutions with different DNA forms could be distinguished by different emission colors, whereas the distinct clear blue emission in the presence of G4-DNA **c-kit**, and **h-ras1** stood out as a special indicative element.

The increased emission intensity of compound **3** after addition of DNA is most likely caused by the limited conformational freedom of the ligand within the DNA binding site,[3b]

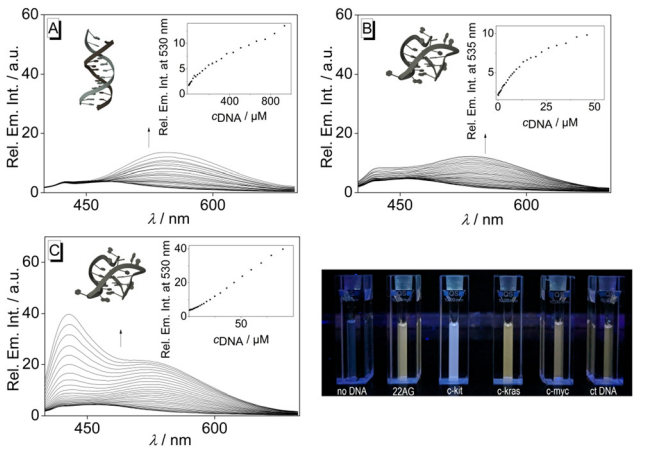

Fig. 3 Fluorimetric titration of **3** (c = 20 μM) with ct DNA (A), **22AG** (B), and **c-kit** (C); (A: in BPE buffer, c_{Na^+} = 16 mM, pH = 7.0, B and C: in K-phosphate buffer, c_{K^+} = 95 mM, pH = 7.0). The arrows indicate the development of the absorption or emission bands during the titration. Inset: plot of the emission at λ = 330 nm or λ = 431 nm *versus* c_{DNA}; of ct DNA (A), **22AG** (B), and **c-kit** (C). Structures in insets taken from the Protein Data Bank (PDB, https://www.rcsb.org/; PDB ID: A, 2k0v; B, 1kf1; C; 6gh0).

which in turn suppresses the torsional relaxation of the biphenyl unit as non-radiative deactivation pathway of the excited molecule. Such a fluorescent light-up effect based on this mechanism has been frequently observed for cationic DNA binders that contain a biaryl substructure.[21] Moreover, this effect of the binding site on the fluorescence properties of the ligand may also explain the varying development of its emission bands upon association with the different DNA forms (Fig. 3). Specifically, the size and shape of the binding sites of the employed DNA forms vary distinctly,[39] so that the bound ligand experiences different degrees of restricted conformational freedom in each case. Such an effect of the binding sites on the emission intensity and energy has already been demonstrated with the structurally resembling compound 9-(4-dimethylamino)benzo[*b*]quinolizinium, which exhibits a fluorescence light-up effect with different emission maxima in duplex and quadruplex DNA.[40] Likewise, this influence of the binding sites on the emission color has been explained by the different conformational flexibility of the ligand within the binding sites.[40]

In the presence of ct DNA, the emission bands resemble the ones in glycerol and indicate the restricted free volume within the DNA binding site, which, in turn, should hinder conformational changes. Accordingly, the relaxation to the non-emissive conformation is suppressed under these conditions. But obviously, minor structural changes to a relaxed TICT/CS state are still possible, so that the related red-shifted emission band is also formed. In contrast, upon binding to G4-DNA a clear dual emission of the bound ligand was observed, which indicates that both the LE state and the TICT/CS state are populated to a significant extent within the respective binding sites. However, as a striking difference the contribution of each emission band varies with the different G4-DNA forms. And in the case of **c-kit** and **h-ras1**, the blue-shifted emission band dominates the overall spectrum, and this combination of bands results in an overall blue emission. For an explanation of this special effect, it is proposed that this effect is caused by the exceptional binding pocket provided by the quadruplex structure.[39c] Specifically, in the case of **c-kit** the particular loop structures allow the formation of a cleft at the 3′-end of the quadruplex in which organic ligands may be accommodated.[41] Indeed, simple docking studies[42] with the ligand **3** and **c-kit** revealed that the biphenyl **3** may bind in this binding pocket (Fig. 4) and point to a suppression of conformational freedom of the biphenyl unit in this constrained environment. As a result, the emission occurs mainly from the LE state leading to a distinct blue emission.[43] Likewise, it is proposed that the conformational flexibility of ligand **3** is similarly restricted in the binding site of **h-ras1**. In this particular case, the available free volume is probably even more confined because the fluorescence light-up factor is larger. The "regular" terminal π stacking of the ligand at the other G4-DNA forms **c-kras**, **c-myc**, **22AG**, by contrast, leaves sufficient conformational freedom to give mainly the red-shifted emission of the relaxed state. Notably, these latter G4-DNA forms have different quadruplex structures regarding the

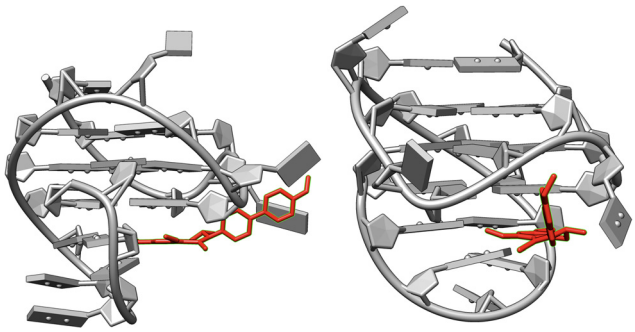

Fig. 4 Structure of the complex between ligand **3** and G4-DNA **c-kit** (PDB ID: 2O3M) as estimated from molecular docking (AutoDock Vina, UCSF Chimera 1.15).

DNA-strand orientation, namely parallel (**c-kras**, **c-myc**) and hybrid (**22AG**); and likewise, the quadruplex forms, with which a more pronounced blue shift was observed, have different strand alignment (**c-kit**: parallel, **h-ras1**: antiparallel). Therefore, it may be concluded that this particular structural parameter does not influence significantly the emission properties of the bound ligand **3**. At the same time, it cannot be excluded that the different polarity and/or availability of hydrogen bonds within the binding sites of the different G4-DNA forms also contributes to the varying emission properties of the bound ligand, because similar effects were observed in different solvents (Fig. 1). In this context, it should be emphasized that the different fluorescence response of the ligand **3** upon association with different DNA forms is not the result of a selective DNA recognition, because the binding studies revealed similar affinities to all tested DNA forms (see above). Instead, the varying emission properties are most likely caused by the different binding modes in combination with the high sensitivity of the dual emission of the biphenyl fluorophore on the surrounding medium.

Conclusions

In summary, we have identified the cationic, donor–acceptor-substituted biphenyl structure **3** as a promising complementary motif of quadruplex DNA binders. It has, to the best of our knowledge, not been introduced to this research field so far. However, biaryl-type fluorophores are already known that may be used for fluorimetric DNA detection, with thioflavin T (ThT) being the most prominent example.[44] But these fluorescent probes do not exhibit dual emission, so that their response to DNA binding is a fluorescence light-up effect *without* a color change.

In the present case, neither the affinity nor the selectivity of the ligand towards a particular DNA form was especially pronounced. But still, the high sensitivity of the emission properties of the biphenyl unit, specifically the pronounced dual emission, to the surrounding medium may be used to detect and characterize different binding sites of G4-DNA by distinct

emission properties of the bound ligand. Specifically, sterically constrained binding sites, such as the one in **c-kit**, may be identified by the characteristic stronger contribution of the blue-shifted emission band. Therefore, it is proposed that similar cationic biphenyl derivatives with optimized structures for stronger binding affinities will figure as useful and efficient tools for the fluorimetric analysis of quadruplex DNA.

Data availability

The data supporting this article have been included as part of the ESI.‡

Conflicts of interest

There are no conflicts to declare.

Acknowledgements

We thank the University of Siegen for financial support. D. S. thanks the *House of Young Talents* (University of Siegen) for a Ph.D. fellowship. We thank Jennifer Hermann, Hannah Karola Strunk, and Sandra Uebach (University of Siegen) for technical assistance.

References

1 (*a*) S. Munan, Y.-T. Chang and A. Samanta, Chronological development of functional fluorophores for bio-imaging, *Chem. Commun.*, 2024, **60**, 501–521; (*b*) R. Zhai, B. Fang, Y. Lai, B. Peng, H. Bai, X. Liu, L. Li and W. Huang, Small-molecule fluorogenic probes for mitochondrial nanoscale imaging, *Chem. Soc. Rev.*, 2023, **52**, 942–972; (*c*) D. B. Sung and J. S. Lee, Natural-product-based fluorescent probes: recent advances and applications, *RSC Med. Chem.*, 2023, **14**, 412–432; (*d*) H. Li, Y. An, J. Gao, M. Yang, J. Luo, X. Li, J. Lv, X. Li, Z. Yuan and H. Ma, Recent Advances of Fluorescence Probes for Imaging of Ferroptosis Process, *Chemosensors*, 2022, **10**, 233–255.

2 (*a*) Y. Li, T. Liu and J. Sun, Recent Advances in *N*-Heterocyclic Small Molecules for Synthesis and Application in Direct Fluorescence Cell Imaging, *Molecules*, 2023, **28**, 733; (*b*) H. Niu, J. Liu, H. M. O'Connor, T. Gunnlaugsson, T. D. James and H. Zhang, Photoinduced electron transfer (PeT) based fluorescent probes for cellular imaging and disease therapy, *Chem. Soc. Rev.*, 2023, **52**, 2322–2357; (*c*) S. Samanta, K. Lai, F. Wu, Y. Liu, S. Cai, X. Yang, J. Qu and Z. Yang, Xanthene, cyanine, oxazine and BODIPY: the four pillars of the fluorophore empire for super-resolution bioimaging, *Chem. Soc. Rev.*, 2023, **52**, 7197–7261; (*d*) D. Cheng, W. Xu, X. Gong, L. Yuan and X.-B. Zhang, Design Strategy of Fluorescent Probes for Live Drug-Induced Acute Liver Injury Imaging, *Acc. Chem. Res.*, 2021, **54**, 403–415; (*e*) C. Guo, A. C. Sedgwick, T. Hirao and J. L. Sessler, Supramolecular fluorescent sensors: An historical overview and update, *Coord. Chem. Rev.*, 2021, **427**, 213560; (*f*) A. Saini, J. Singh and S. Kumar, Optically superior fluorescent probes for selective imaging of cells, tumors, and reactive chemical species, *Org. Biomol. Chem.*, 2021, **19**, 5208; (*g*) Y. V. Suseela, N. Narayanaswamy, S. Pratihar and T. Govindaraju, Far-red fluorescent probes for canonical and non-canonical nucleic acid structures: current progress and future implications, *Chem. Soc. Rev.*, 2018, **47**, 1098–1131.

3 (*a*) J. Gebhard, L. Hirsch, C. Schwechheimer and H.-A. Wagenknecht, Hybridization-Sensitive Fluorescent Probes for DNA and RNA by a Modular "Click" Approach, *Bioconjugate Chem.*, 2022, **33**, 1634–1642; (*b*) S. B. Wagh, V. A. Maslivetc, J. La Chair and A. Kornienko, Lessons in Organic Fluorescent Probe Discovery, *ChemBioChem*, 2021, **22**, 3109–3139; (*c*) A. Granzhan, H. Ihmels and M. Tian, The benzo[*b*]quinolizinium ion as a water-soluble platform for the fluorimetric detection of biologically relevant analytes, *ARKIVOC*, 2015, 494–523.

4 H. Tateishi-Karimata and N. Sugimoto, Chemical biology of non-canonical structures of nucleic acids for therapeutic applications, *Chem. Commun.*, 2020, **56**, 2379–2390.

5 (*a*) K. Weisz, A world beyond double-helical nucleic acids: the structural diversity of tetra-stranded G-quadruplexes, *ChemTexts*, 2021, **7**, 25; (*b*) Y. Xu, Chemistry in human telomere biology: structure, function and targeting of telomere DNA/RNA, *Chem. Soc. Rev.*, 2011, **40**, 2719–2740.

6 (*a*) J. Jana and K. Weisz, Thermodynamic Stability of G-Quadruplexes: Impact of Sequence and Environment, *ChemBioChem*, 2021, **22**, 2848–2856; (*b*) M. Sanderson and S. Neidle, *Principles of Nucleic Acid Structure*, Academic Press, 2nd edn, 2021.

7 G. W. Collie and G. N. Parkinson, The application of DNA and RNA G-quadruplex to therapeutic medicines, *Chem. Soc. Rev.*, 2011, **40**, 5867–5892.

8 A. Verma, V. K. Yadav, R. Basundra, A. Kumar and S. Chowdhury, Evidence of genome-wide G4 DNA-mediated gene expression in human cancer cells, *Nucleic Acids Res.*, 2009, **37**, 4194–4204.

9 X. Xie, M. Zuffo, M.-P. Teulade-Fichou and A. Granzhan, Identification of optimal fluorescent probes for G-quadruplex nucleic acids through systematic exploration of mono- and distyryl dye libraries, *Beilstein J. Org. Chem.*, 2019, **15**, 1872–1889.

10 (*a*) L.-S. Rao, L. Hao, L.-Y. Liu, Y.-L. Zeng, B.-B. Liang, W. Liu and Z.-W. Mao, Detection and tracking of cytoplasmic G-quadruplexes in live cells, *Chem. Commun.*, 2023, **59**, 13348–13351; (*b*) H. Yang, Y. Zhou and J. Liu, G-quadruplex DNA for construction of biosensors, *TrAC, Trends Anal. Chem.*, 2020, **132**, 116060; (*c*) P. Chilka, N. Desai and B. Datta, Small Molecule Fluorescent Probes for G-Quadruplex Visualization as Potential Cancer Theranostic Agents, *Molecules*, 2019, **24**, 752.

11 M. Zuffo, X. Xie and A. Granzhan, Strength in Numbers: Development of a Fluorescence Sensor Array for Secondary Structures of DNA, *Chem. – Eur. J.*, 2019, **25**, 1812–1818.

12 (*a*) J.-N. Han, C. Zhong, M. Ge, S. Kuang and Z. Nie, Engineering fluorescent protein chromophores with an internal reference for high-fidelity ratiometric G4 imaging in living cells, *Chem. Sci.*, 2023, **14**, 4538–4548; (*b*) A. S. Oshchepkov, O. Reznichenko, D. Xu, B. S. Morozov, A. Granzhan and E. A. Kataev, Dye-functionalized phosphate-binding macrocycles: from nucleotide to G-quadruplex recognition and "turn-on" fluorescence sensing, *Chem. Commun.*, 2021, **57**, 10632–10635.

13 X. Xie, B. Choi, E. Largy, R. Guillot and A. Granzhan, Asymmetric Distyrylpyridinium Dyes as Red-Emitting Fluorescent Probes for Quadruplex DNA, *Chem. – Eur. J.*, 2013, **19**, 1214–1226.

14 L. Chen, J. Dickerhoff, S. Sakai and D. Yang, DNA G-Quadruplex in Human Telomeres and Oncogene Promoters: Structures, Functions, and Small Molecule Targeting, *Acc. Chem. Res.*, 2022, **55**, 2628–2646.

15 R. Sun, X. Guo, D. Yang, Y. Tang, J. Lu and H. Sun, c-Myc G-quadruplex is sensitively and specifically recognized by a fluorescent probe, *Talanta*, 2021, **226**, 122125.

16 (*a*) H.-Z. He, K. Li, K.-K. Yu, P.-L. Lu, M.-L. Feng, S.-Y. Chen and X.-Q. Yu, Additive- and column-free synthesis of rigid bis-coumarins as fluorescent dyes for G-quadruplex sensing *via* disaggregation-induced emission, *Chem. Commun.*, 2020, **56**, 6870–6873; (*b*) M. Deiana, K. Chand, J. Jamroskovic, I. Obi, E. Chorell and N. Sabouri, A Light-up Logic Platform for Selective Recognition of Parallel G-Quadruplex Structures via Disaggregation-Induced Emission, *Angew. Chem., Int. Ed.*, 2020, **59**, 896–902.

17 A. T. Phan, V. Kuryavyi, S. Burge, S. Neidle and D. J. Patel, Structures of an Unprecedented G-Quadruplex Scaffold in the Human *c-kit* Promoter, *J. Am. Chem. Soc.*, 2007, **129**, 4386–4392.

18 G. Bringmann, T. Gulder, B. Hertlein, Y. Hemberger and F. Meyer, Total Synthesis of the *N,C*-Coupled Naphthylisoquinoline Alkaloids Ancistrocladinium A and B and Related Analogues, *J. Am. Chem. Soc.*, 2010, **132**, 1151–1158.

19 (*a*) J. L. Belmonte-Vazquez, Y. A. Amador-Sanchez, L. A. Rodriguez-Cortes and B. Rodriguez-Molina, Dual-State Emission (DSE) in Organic Fluorophores: Design and Applications, *Chem. Mater.*, 2021, **33**, 7160–7184; (*b*) C. Wang, W. Chi, Q. Qiao, D. Tan, Z. Xu and X. Liu, Twisted intramolecular charge transfer (TICT) and twists beyond TICT: from mechanisms to rational designs of bright and sensitive fluorophores, *Chem. Soc. Rev.*, 2021, **50**, 12656–12678.

20 (*a*) C. Chen and C. Fang, Fluorescence Modulation by Amines: Mechanistic Insights into Twisted Intramolecular Charge Transfer (TICT) and Beyond, *Chemosensors*, 2023, **11**, 87; (*b*) M. Wang, R.-Z. Wang and C.-H. Zhao, Temperature-Dependent Dual Fluorescence from Small Organic Molecules, *Org. Mater.*, 2022, **4**, 204–215; (*c*) S. K. Behera, S. Y. Park and J. Gierschner, Dual Emission: Classes, Mechanisms, and Conditions, *Angew. Chem., Int. Ed.*, 2021, **60**, 22624–22638; (*d*) S. Sasaki, G. P. C. Drummen and G.-i. Konishi, Recent advances in twisted intramolecular charge transfer (TICT) fluorescence and related phenomena in materials chemistry, *J. Mater. Chem. C*, 2016, **4**, 2731–2743; (*e*) V. V. Volchkov and B. M. Uzhinov, Structural relaxation of excited molecules of heteroaromatic compounds, *High Energy Chem.*, 2008, **42**, 153–169; (*f*) Z. R. Grabowski, K. Rotkiewicz and W. Rettig, Structural Changes Accompanying Intramolecular Electron Transfer: Focus on Twisted Intramolecular Charge-Transfer States and Structures, *Chem. Rev.*, 2003, **103**, 3899–4032.

21 M. Tian and H. Ihmels, Synthesis of Fluorescent 9-Aryl-Substituted Benzo[*b*]quinolizinium Derivatives, *Synthesis*, 2009, **24**, 4226–4234.

22 S. Nigam and S. Rutan, Principles and Applications of Solvatochromism, *Appl. Spectrosc.*, 2001, **55**, 362A–370A.

23 S. I. Druzhinin, S. R. Dubbaka, P. Knochel, S. A. Kovalenko, P. Mayer, T. Senyushkina and K. A. Zachariasse, Ultrafast Intramolecular Charge Transfer with Strongly Twisted Aminobenzonitriles: 4-(Di-*tert*-butylamino)benzonitrile and 3-(Di-*tert*-butylamino)benzonitrile, *J. Phys. Chem. A*, 2008, **112**, 2749–2761.

24 (*a*) M. M. Sreejaya, V. M. Pillai, A. Ayesha, M. Baby, M. Bera and M. Gangopadhyay, Mechanistic analysis of viscosity-sensitive fluorescent probes for applications in diabetes detection, *J. Mater. Chem. B*, 2024, **12**, 2917–2937; (*b*) H. Xiao, P. Li and B. Tang, Small Molecular Fluorescent Probes for Imaging of Viscosity in Living Biosystems, *Chem. – Eur. J.*, 2021, **27**, 6880–6898; (*c*) M. Vogel and W. Rettig, Efficient Intramolecular Fluorescence Quenching in Triphenylmethane-Dyes Involving Excited States with Charge Separation and Twisted Conformations, *Ber. Bunsenges. Phys. Chem.*, 1985, **89**, 962–968.

25 M. Vogel and W. Rettig, Efficient Intramolecular Fluorescence Quenching in Triphenylmethane-Dyes Involving Excited States with Charge Separation and Twisted Conformations, *Ber. Bunsenges. Phys. Chem.*, 1985, **89**, 962–968.

26 T. Förster and G. Hoffmann, Die Viskositätsabhängigkeit der Fluoreszenzquantenausbeuten einiger Farbstoffsysteme, *Z. Phys. Chem.*, 1971, **75**, 63–76.

27 (*a*) K. B. Wang, Y. Liu, J. Li, C. Xiao, Y. Wang, W. Gu, Y. Li, Y. Z. Xia, T. Yan, M. H. Yang and L. Y. Kong, Structural insight into the bulge-containing *KRAS*, oncogene promoter G-quadruplex bound to berberine and coptisine, *Nat. Commun.*, 2022, **13**, 6016; (*b*) M. Sanderson and S. Neidle, *Principles of Nucleic Acid Structure*, Academic Press, 2nd edn, 2021; (*c*) A. T. Phan, V. Kuryavyi, S. Burge, S. Neidle and D. J. Patel, Structure of an Unprecedented G-Quadruplex Scaffold in the Human *c-kit* Promoter, *J. Am. Chem. Soc.*, 2007, **129**, 4386–4392.

28 F. H. Stootman, D. M. Fisher, A. Rodger and J. R. Aldrich-Wright, Improved curve fitting procedures to determine equilibrium binding constants, *Analyst*, 2006, **131**, 1145–1151.

29 B. Nordén, A. Rodger and T. Dafforn, *Linear Dichroism and Circular Dichroism: A Textbook on Polarized-Light Spectroscopy*, RSC Publishing, Cambridge, 2010.
30 M. M. Aleksić and V. Kapetanović, An Overview of the Optical and Electrochemical Methods for Detection of DNA-Drug Interactions, *Acta Chim. Slov.*, 2014, **61**, 555–573.
31 (*a*) F. Nagatsugi and K. Onizuka, Functional G-Quadruplex Binding Molecules, *Chem. Lett.*, 2020, **49**, 771–780; (*b*) M. P. O'Hagan, J. C. Morales and M. C. Galan, Binding and Beyond: What Else Can G-Quadruplex Ligands Do?, *Eur. J. Org. Chem.*, 2019, 4995–5017.
32 T. M. Aliyeu, D. V. Berdnikova, O. A. Fedorova, E. N. Gulakova, C. Stremmel and H. Ihmels, Regiospecific Photocyclization of Mono- and Bis-Styryl-Substituted N-Heterocycles: A Synthesis of DNA-Binding Benzo[*c*]quinolizinium Derivatives, *J. Org. Chem.*, 2016, **81**, 9075–9085.
33 (*a*) P. Bosch, G. Marcelo, A. Matamoros-Recio, D. Sucunza, F. Mendicuti, A. Domingo and J. J. Vaquero, A new family of fluorescent pyridazinobenzimidazolium cations with DNA binding properties, *Dyes Pigm.*, 2021, **192**, 109443; (*b*) A. K. Das, H. Ihmels and S. Kölsch, Diphenylaminostyryl-substituted quinolizinium derivatives as fluorescent light-up probes for duplex and quadruplex DNA, *Photochem. Photobiol. Sci.*, 2019, **18**, 1373–1381.
34 V. Pirota, M. Stasi, A. Benassi and F. Doria, Chapter Six – An overview of quadruplex ligands: Their common features and chemotype diversity, *Annu. Rep. Med. Chem.*, 2020, **54**, 163–196.
35 I. Frasson, V. Pirota, S. N. Richter and F. Doria, Multimeric G-quadruplexes: A review on their biological roles and targeting, *Int. J. Biol. Macromol.*, 2022, **204**, 89–102.
36 A. De Cian, L. Guittat, M. Kaiser, B. Sacca, S. Amrane, A. Bourdoncle, P. Alberti, M.-P. Teulade-Fichou, L. Lacroix and J.-L. Mergny, Fluorescence-based melting assay for studying quadruplex ligands, *Methods*, 2007, **42**, 183–195.
37 J. Becher, D. V. Berdnikova, H. Ihmels and C. Stremmel, Synthesis and investigation of quadruplex-DNA-binding, 9-*O*-substituted berberine derivatives, *Beilstein J. Org. Chem.*, 2020, **16**, 2795–2806.
38 Y. Zhang, Y. Cheng, Q. Luo, T. Wu, J. Huo, M. Yin, H. Peng, Y. Xiao, Q. Tong and H. You, Distinguishing G-Quadruplexes Stabilizer and Chaperone for c-*MYC* Promoter G-Quadruplexes through Single-Molecule Manipulation, *J. Am. Chem. Soc.*, 2024, **146**, 3689–3699.
39 (*a*) K.-B. Wang, Y. Liu, J. Li, C. Xiao, Y. Wang, W. Gu, Y. Li, Y.-Z. Xia, T. Yan, M.-H. Yang and L.-Y. Kong, Structural insight into the bulge-containing *KRAS* oncogene promoter G-quadruplex bound to berberine and coptisine, *Nat. Commun.*, 2022, **13**, 6016; (*b*) J. Spiegel, S. Adhikari and S. Balasubramanian, The Structure and Function of DNA G-Quadruplexes, *Trends Chem.*, 2020, **2**, 123–136; (*c*) D. Wei, G. N. Parkinson, A. P. Reszka and S. Neidle, Crystal structure of a c–*kit* promoter quadruplex reveals the structure role of metal ions and water molecules in maintaining loop conformation, *Nucleic Acids Res.*, 2012, **40**, 4691–4700.
40 R. Bortolozzi, H. Ihmels, L. Thomas, M. Tian and G. Viola, 9-(4-Dimethylaminophenyl)benzo[*b*]quinolizinium: A Near-Infrared Fluorophore for the Multicolor Analysis of Proteins and Nucleic Acids in Living Cells, *Chem. – Eur. J.*, 2013, **19**, 8736–8741.
41 (*a*) K. G. Moghaddam, A. H. de Vries, S. J. Marrink and S. Faraji, Binding of quinazolinones to c-KIT G-quadruplex; an interplay between hydrogen bonding and π-π stacking, *Biophys. Chem.*, 2019, **253**, 106220; (*b*) A. Głuszyńska, B. Juskowiak, M. Kuta-Siejkowska, M. Hoffmann and S. Haider, Carbazole Derivatives Binding to c-KIT G-Quadruplex DNA, *Molecules*, 2018, **23**, 1134–1154; (*c*) D. Wei, J. Husby and S. Neidle, Flexibility and structural conversation in a c-KIT G-quadruplex, *Nucleic Acids Res.*, 2015, **43**, 629–644; (*d*) A. T. Phan, V. Kuryavyi, S. Burge, S. Neidle and D. J. Patel, Structure of an Unprecedented G-Quadruplex Scaffold in the Human *c-kit* Promoter, *J. Am. Chem. Soc.*, 2007, **129**, 4386–4392.
42 O. Trott and A. J. Olson, AutoDock Vina: Improving the speed and accuracy of docking with a new scoring function, efficient optimization, and multithreading, *J. Comput. Chem.*, 2009, **31**, 455–461.
43 (*a*) A. Pandith, U. Nagarajachari, R. K. G. Siddappa, S. Lee, C.-J. Park, K. Sannathammegowda and Y. J. Seo, Loop-mediated fluorescent probes for selective discrimination of parallel and antiparallel G-Quadruplexes, *Bioorg. Med. Chem.*, 2021, **35**, 116077; (*b*) V. Dhamodharan and P. I. Pradeepkumar, Specific Recognition of Promoter G-Quadruplex DNAs by Small Molecule Ligand and Light-up Probes, *ACS Chem. Biol.*, 2019, **14**, 2102–2114.
44 (*a*) R.-X. Wang, Y. Ou, Y. Chen, T.-B. Ren, L. Yuan and X.-B. Zhang, Rational Design of NIR-II G-Quadruplex Fluorescent Probes for Accurate In Vivo Tumor Metastasis Imaging, *J. Am. Chem. Soc.*, 2024, **146**, 11669–11678; (*b*) M. Lv, J. Ren and E. Wang, Topological effect of an intramolecular split G-quadruplex on thioflavin T binding and fluorescence light-up, *Chem. Sci.*, 2024, **15**, 4519–4528; (*c*) S. Liu, P. Peng, H. Wang, L. Shi and T. Li, Thioflavin T binds dimeric parallel-stranded GA-containing non-G-quadruplex DNAs: a general approach to lighting up double-stranded scaffolds, *Nucleic Acids Res.*, 2017, **45**, 12080–12089; (*d*) Q. Xu, M. Yang, Y. Chang, S. Peng, D. Wang, X. Zhou and Y. Shao, Switching G-quadruplex to parallel duplex by molecular rotor clustering, *Nucleic Acids Res.*, 2022, **50**, 10249–10263; (*e*) R. Kumar, K. Chand, S. Bhowmik, R. N. Das, S. Bhattacharjee, M. Hedenström and E. Chorell, Subtle structural alterations in G-quadruplex DNA regulate site specificity of fluorescence light-up probes, *Nucleic Acids Res.*, 2020, **48**, 1108–1119.